Materials Science-Poland, Vol. 22, No. 1, 2004

Analysis of ionisation energies of ions, ionic radii in a crystal lattice and the energy of electrons in ionic cores of metal atoms

ANDRZEJ STOKŁOSA*, JANUSZ ZAJĘCKI, STEFAN S. KUREK

Cracow University of Technology, Institute of Chemical Engineering and Physical Chemistry, ul. Warszawska 24, 31-155 Kraków, Poland

An analysis of ionic radii, ionisation energies of ions and the electron binding energies in the highest occupied atomic orbitals of elements in their thermodynamically stable states is presented in the paper. It was shown that, for a number of ions of the same electronic configuration, several parameters, like the reciprocals of the ionic radii, square roots of ionisation energies and electron binding energies, are linear functions of the nuclear charge of ion (atomic number). A formal agreement of the character of the obtained relationships with the Slater equations describing the energies and the radii of electronic shells in atoms allows us to treat the constants in the obtained equations as an 'empirical' effective main quantum number and an 'empirical' screening constant.

Key words: *ion ionisation energy; electron binding energy; ionic radius*

1. Introduction

The development of modern chemistry, lasting for 150 years, in principle began with the discovery of periodic changes in properties of elements leading to the formulation of the periodicity law and the periodic table of elements. Advances in quantum chemistry allow us to determine quite precisely the electronic structures of atoms, the geometries of molecules and atomic interactions in molecules containing a significant number of atoms. One can even calculate interactions in solid state fragments comprising several tens of atoms by these methods. The density functional theory (DFT) proved to be the most successful in this area [1]. DFT calculations yield parameters of great importance to the materials chemistry. A simple concept of electronegativity can

*Corresponding author, e-mail: astoklos@chemia.pk.edu.pl.

be employed for the prediction of the stability of alloys, both electronegativity and hardness are applied in the calculation of the surface atoms properties, hence in explaining and predicting adsorption in such applications as catalysis and adhesion, just to name a few examples. DFT also enables one to obtain parameters of atoms on solid surfaces. It has also given, both chemical and physical, clear definitions of such paramount parameters as electronegativity and hardness of atoms and ions [2]. On the other hand, advances in experimental techniques and data obtained by these methods enable in many cases the theoretical models to be verified. They provide data on electron interaction energies not only in isolated atoms but also in atoms in crystalline structures. In spite of this great progress in gaining information concerning molecules and solid state structures, periodic changes in the properties of ions have remained a very important scientific problem. Approximate but simple correlations between relatively easily available values (such as the ionisation energy, the binding energies of electrons in given shells or the ionic radii and changes in properties of compounds formed by these ions) are very important in many areas of materials science, such as mineralogy, ceramics and metallurgy, in which the above parameters are sufficient to predict the geometries and properties of quite complex systems. It still remains open to what extent the complexity of the interactions of atoms in molecules or in crystal lattices changes their properties compared to the parent atoms or isolated ions or how it differentiates atom properties (in general depending on their surrounding).

One of the values characterising atoms and isolated (free) ions is their ionisation energy, a value that determines the energy with which an electron interacts with the atomic core containing a nucleus and the remaining electrons. The energy of the highest occupied Kohn–Sham orbital, used in DFT, will approach the negative of the first ionisation potential exactly [3]. Another similar value is the electron binding energy in the outermost filled electronic shell in atoms of elements in their thermodynamically stable forms. This energy characterises the atom core, the ‘ion core’ with valence electrons removed, in a state in which the atoms form metallic bonding in metals or atomic (homoatomic) bonding, for example, in the gas phase or in crystals of non-metals. The above parameters have an important feature of being absolute values, not derived from any models, and due to advances in spectroscopic methods are determined accurately.

Another parameter which defines the space occupied by an atom or an ion in a crystal is its radius, whose value can be estimated by various methods. Although it does not have any precisely defined physical sense, it allows us to formulate a useful working hypothesis, often employed in solutions of various problems in solid state chemistry. The concept of ionic radius is linked to an ion of a determined electric charge occurring in a crystal with dominating ionic interactions. It is therefore important to define the space occupied by the ion, i.e., the atom nucleus along with the electrons filling the electronic shells. The radius of the atom core is also used as a value of the ionic radius. Therefore, what is determined is the ‘radius’ of the outermost shell of, for example, C^{4+} or S^{6+} ions.

The ionisation potential of ions is employed in the discussion of variation of the properties of solids. Ionic radii, determined for ions in crystal lattices, are often used in analyses of isolated ions. Swapping the values obtained for isolated ions with those obtained for ions in crystal lattices would be justified, provided that the differences between ions in such different environments were insignificant, which is generally not true.

In the present work, in spite of tremendous progress in quantum chemistry (particularly DFT), we would return to the problems mentioned above. Based on the values of ionic radii, which have been refined many times, and on accurately defined ion ionisation energies, we present their analysis. The aim of the analysis is to point out the differences between ions of the same electron configurations in various states and environments.

2. Ion ionisation enthalpy

Isolated ions have unperturbed structures. They can be quite precisely characterised due to the possibility of determining the energies of individual ionisation stages. For the analysis of the ionisation energies of ions of various charges, we have employed the enthalpy of their ionisation. The compiled results of several authors presented in handbooks and monographs [4–7] were the data source. Figure 1 presents a correlation between the nuclear charge of ion Z and the square root of its ionisation energy, E_{IE}, divided by the Rydberg constant R (in the Rydberg's units). For example, for the Al^{3+} ion, we took the fourth degree of ionisation of the aluminium atom.

The above correlation is presented for ions of the 2- and 10-electron configurations, for the 18- through 25-electron configurations, and for the remaining electron configurations in Figs. 1a–c. As can be seen in Figs. 1a and 1c, the above relationship is linear for a number of ions having the electron configurations of noble gases and the configuration of Ni (28 electrons), Pd (54), Pt (78) (with filled outermost (sp) shells and (d) subshells, respectively). This can be expressed by an equation of the general form

$$Z = a_{IE}\sqrt{\frac{E_{IE}}{R}} + S_{IE} \tag{1}$$

Figure 1b, in turn, presents this relationship for the ionisation enthalpy of ions of unfilled valence (d) subshells. As can be seen, analogous linear relationships were obtained for ions of the same configuration and, what is more, of approximately the same slope as the line representing the 18-electron configuration. It should be noted that for a number of ions which do not occur as free ions, or in oxidation states that are even not postulated, the $\sqrt{E_{IE}/R}$ values are located on extensions of the obtained lines or only slightly deviate from them. This includes, for example, Fe^{5+}, Fe^{6+}, Fe^{7+} or higher oxidation states of Co and Ni ions.

In Figures 1a–c, the values of ionisation enthalpies of simple anions were shown for comparison, extracted from available data for electron affinities [4, 7, 8]. As can

Table 1. Parameters a_n and S_n^* of Eq. (1) for ions of the same electronic configuration of N_c electrons

Electronic configuration	Number of electrons of configuration N_c	Parameters of Eq. (1) for ionisation enthalpy of ions			Parameters of Eq. (1) for electron binding energy			Effective principal quantum number, n^*	Slater screening constant S_s
		Series of ions	a_{IE}	S_{IE}	Series of ions	a_{EBE}	S_{EBE}		
$1s^2$	2	Li^+–F^{7+}	0.996	0.652	Li^+–F^{7+}	1.164	0.661	1.000	0.3
2(sp)	10	Na^+–S^{6+}	1.868	7.479	Na^+–Cl^{7+}	2.550	7.132	2.000	4.15
2(sp)	10	N^3–F^-	–3.311	10.655					
$3s^2$	12	Si^{2+}–Cl^{5+}	2.724	9.714					
$3s^2p^2$	14	S^{2+}–Cl^{3+}	2.609	11.827					
3(sp)	18	K^+–Mn^{7+}	2.662	14.861	K^+–Ca^{2+}	4.839	13.386	3.000	11.25
3(sp)	18				Sc^{3+}–Mn^{7+}	9.485	7.312		
3(sp)	18	S^2–Cl^-	–8.260	21.262					
$3(sp)d^1$	19	V^{4+}–Cr^{5+}	2.485	17.599					
$3(sp)d^2$	20	Ti^{2+}–Mn^{5+}	2.442	18.503					
$3(sp)d^3$	21	V^{2+}–Mn^{4+}	2.382	19.492					
$3(sp)d^4$	22	Cr^{2+}–Fe^{4+}	2.380	20.401					
$3(sp)d^5$	23	Mn^{2+}–Co^{4+}	2.368	21.265					
$3(sp)d^6$	24	Fe^{2+}–Ni^{4+}	2.315	22.518					
$3(sp)d^7$	25	Co^{2+}–Ni^{4+}	2.271	23.436					
$3(sp)d^{10}$	28	Cu^+–Se^{6+}	2.278	26.121	Zn^{2+}–Br^{7+}	3.589	26.813		21.85
$4s^2$	30	Ge^{2+}–Br^{5+}	3.105	27.057					
$4s^2p^2$	32	Se^{2+}–Br^{3+}	2.787	29.804					
4(sp)	36	Rb^+–Mo^{6+}	3.087	32.548	Rb^+–Sr^{2+}	6.449	30.159	3.700	27.75
4(sp)	36				Y^{3+}–Mo^{6+}	9.635	26.356		
4(sp)	36				Tc^{7+}–Rh^{9+}	13.353	20.147		
$5s^2$	38	Zr^{2+}–Mo^{4+}	2.845	36.276					
$4(sp)d^3$	39	Nb^{2+}–Mo^{3+}	2.037	38.235					
$4(sp)d^{10}$	46	Ag^+–Te^{6+}	2.602	43.74	Cd^{2+}–Sn^{4+}	4.557	43.946		39.45
$4(sp)d^{11}$	46				Sb^{5+}–I^{7+}	5.554	42.454		
$5s^2$	48	Sn^{2+}–Te^{4+}	3.441	44.831					
5(sp)	54	Cs^+–La^{3+}	3.395	50.496	Cs^+–La^{3+}	11.751	43.865	4.000	45.75
$5(sp)d^1$	55	La^{2+}–Pr^{4+}	2.299	54.254					
$5(sp)d^{10}$	78	Au^+–Bi^{5+}	3.025	75.244	Hg^{2+}–At^{7+}	5.291	75.959		71.85
$6s^1$	79	Hg^+–Tl^{2+}	3.262	76.168					
$6s^2$	80	Tl^+–Bi^{3+}	3.336	76.903					

*Subscript n at constants denotes the values obtained by means of ionisation enthalpy (IE) and electron binding energy (EBE) at the outermost filled shell in atoms of elements in their natural form.

be seen, the $\sqrt{E_{IE}/R}$ values computed for anions show a deviation from the line determined for cations of the same electron configuration. Monovalent anions have values lower than those obtained from linear extrapolation, which indicates that electrons in isolated anions are bound relatively weaker than in cations of the same configuration. It should be emphasised that when a first electron is added to an atom the energetic effect is exothermic (anion ionisation potential has the same sign as in the case of cations), whereas adding the second electron is an endothermic process. Since the ionisation enthalpies of divalent anions are negative, the absolute values of $|E_{IE}|$ for anions were plotted in Fig. 1 merely for illustration.

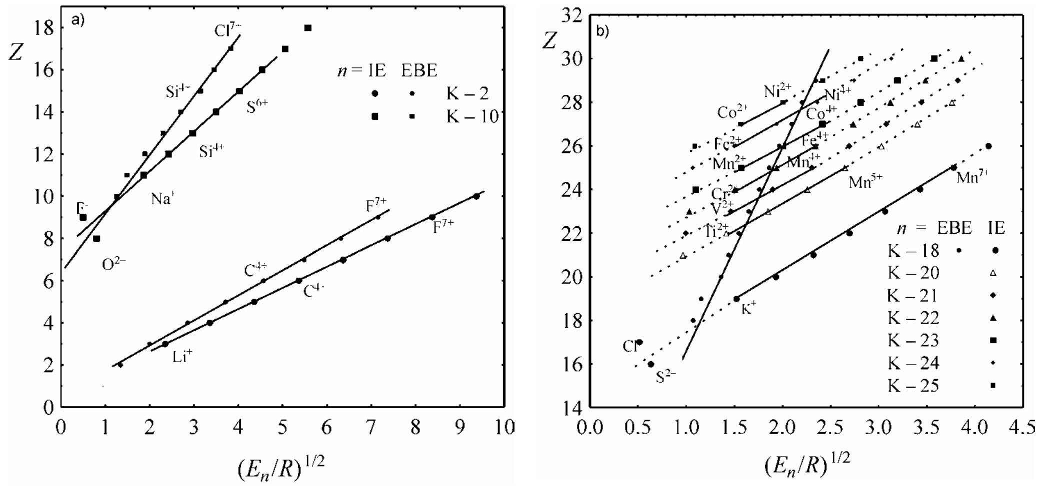

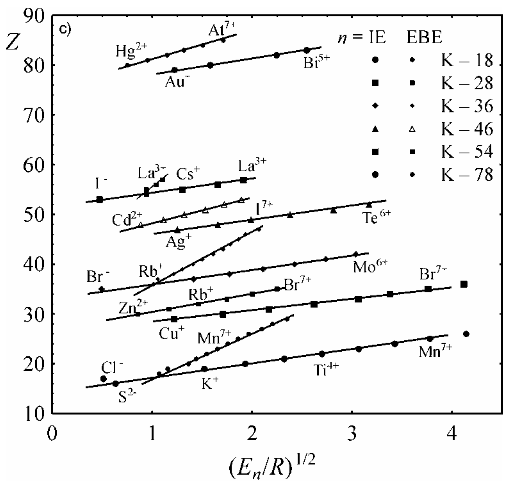

Fig. 1. Correlation between the nuclear charge of ion, Z, and the square root of ionisation enthalpy, E_{IE} (in Rydberg's units) of M^{z+} ions (ionisation degree $(z + 1)$) – filled points, and electron binding energy (E_{EBE}) in the shells corresponding to the outermost filled shell in atoms of elements (in their thermodynamically stable phases) – open points: a) for ions of He (K–2) and Ne (K–10) electron configurations, b) from K–18 to K–25 electron configuration, c) rare gas atom configuration: Ar (K–18), Kr – (K–36), Xe – (K –54) and the atoms of elements: Ni – (K–28), Pd – (K–46), Pt – (K–78)

In Figure 2, the dependence of the parameter a_n on the number of electrons, N_c, in the given configurations is presented (the values of parameters a_n for anions were not plotted in the figure). The symbols of elements shown next to the points denote series of ions of the same electron configuration taken for the calculation of the straight-line parameters. As can be seen from Fig. 2a, the value of the parameter a_{IE} is close to unity for two-electron configuration, whereas it ranges principally between 2 and 3 for the remaining configurations. It can also be noticed that the points representing ions of noble gas configurations are set along a broken line (18, 36 and 54 electron configurations), whereas the points for ions of 28-, 46- and 78-electron configurations (Ni, Pd and Pt ion configurations) are set along a parallel line, significantly shifted. Other configurations stray away from the above lines.

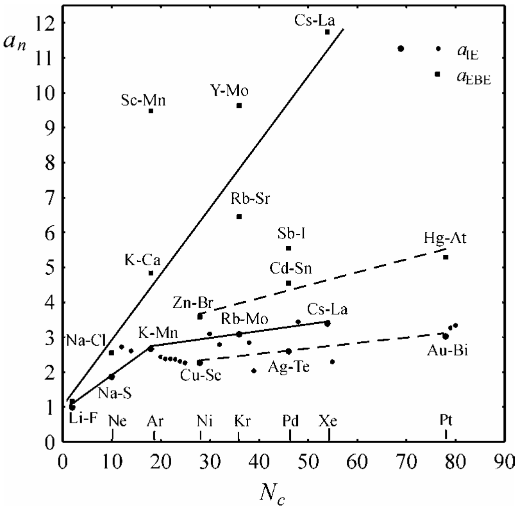

Fig. 2. Dependence of the coefficients a_{IE} and a_{EBE} of Eq. (1) on the number of electrons N_c of respective electron configurations. The circles were based on ionisation enthalpies of ions, the squares were based on electron binding energy in the outermost filled shell (corresponding to the outermost shell of isolated ion) in atoms in their thermodynamically stable phases

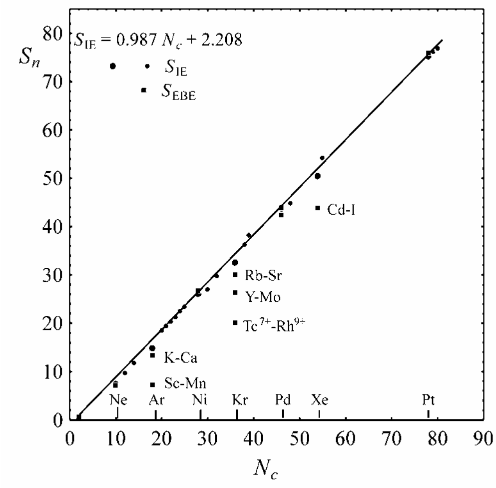

Fig. 3. Dependence of the coefficients S_{IE} and S_{EBE} (Eq. (1)) on the number of electrons N_c of respective electron configurations. The circles were based on ionisation enthalpies of ions, the points were based on electron binding energies in the outermost filled shells (corresponding to the outermost shell of isolated ion) in atoms in their thermodynamically stable phases

Figure 3 presents the dependence of the parameter S_{IE} on the number of electrons of respective electron configurations. As can be seen, the relation is practically linear and can be described by the equation:

$$S_{IE} = 0.987N_c + 2.208 \quad (2)$$

The parameters of the Eq. (2) were determined on the basis of the S_{IE} values for ions of noble gas configurations as well as for ions of the configurations of Ni, Pd and Pt atoms. As can be seen, the values of S_{IE} for other configurations do not lie far away from the above line.

3. Electron binding energy

Ionic cores (atoms stripped of valence electrons) in metals have analogous electron configurations as the ions discussed above. It is often believed that their properties are not very different from those of isolated ions. A value that characterises the ionic core in metals is the electron binding energy in the outermost filled shell of atoms of elements in their thermodynamically stable states (i.e., the states in which the cations stripped of their valence electrons are ‘bonded’ by metallic bonds). The above energy should be close to ionisation energies of ions with filled (sp) shells or (d) subshells. For comparison, the binding energies of electrons in the shell which corresponds to the outermost shell of the above discussed isolated ions was plotted in Fig. 1 (data were taken from the literature [9–12]). The electron binding energies were determined for the elements in their natural form, hence neither for isolated ions, nor for ions in an ionic crystal. As can be seen in the figure, the dependences of the electron binding energies in a given shell, $\sqrt{E_{IE}/R}$, on Z, for various elements also exhibit a linear character in the discussed system of coordinates, but with a different slope. These divergences are quite obvious and result from the fact that the energy of electrons in the outermost filled shell is affected by interactions of covalent or metallic character occurring between atoms. It can therefore be seen that an electron in the 'ion core' in a metal is significantly weaker linked to the nucleus than an analogous electron in the outermost shell in an isolated ion, though it is generally assumed that electrons in (sp) shells do not take part in metallic bonding. A similar situation occurs in the case of molecules with atomic bonds. The linear character of the discussed relationship, presented in Figs. 1a–c, allows us to determine the parameters of linear equations such as Eq. (1). For some configurations though, the relationship was approximated by two or even three linear equations. In Figures 2 and 3, the dependences of those parameters on the number of electrons in the respective electron configurations are presented. As can be seen in the figures, the values of parameters a_{EBE} and S_{EBE}, compared to the analogous parameters based on the ionisation enthalpy, demonstrate quite large differences. This shows that the state of an isolated ion is considerably different from the state of 'ionic' core of atoms of elements in their thermodynamically stable states. It specially refers to the parameters determined for a series of ions of higher charge, like Sc^{3+}–Mn^{7+}, Y^{3+}–Mo^{6+}, Tc^{7+}–Rh^{9+}, Cd^{2+}–I^{7+}.

It results from the presented analysis that differences between the binding energies of electrons in the outermost filled shells of atoms and ion ionisation potentials are so large that they cannot be interchanged in calculations.

4. Slater equations

The linear character of the dependence of ionisation enthalpy on the nuclear charge of ion obtained above is analogous to the Slater equation allowing one to calculate the energy of electronic shells in atoms [13–15]:

$$E_S \frac{R(Z-S)^2}{\left(n^*\right)^2} \tag{3}$$

where: E_S is the energy of a Slater orbital, $R = m_e e^4/\ 8\pi^2\varepsilon_0^2\hbar = 13.5984$ eV is the Rydberg constant, Z is nuclear charge, S is screening constant, n^* stands for the effective main quantum number. The values of the main quantum number given by Slater for the respective shells allow a better agreement between results of quantum-mechanical calculations and those obtained from experiments to be achieved. By rearranging the above equation, we get a relationship which is analogous to Eq. (1):

$$Z = n^{*}\sqrt{\frac{E_{S}}{R}} + S \tag{4}$$

It results from comparing Eqs. (1) and (4) that the proportionality coefficient a_{IE} can be treated as a parameter corresponding to the effective principal quantum number and the parameter S_{IE} as a screening constant. The agreement is quite good, particularly because the values S_S calculated on the basis of the Slater rules yield correct shell energies for elements with the atomic number lower than 18.

Quite large differences between the parameters a_n and S_n based on the electron binding energy in an appropriate shell and the ionisation enthalpy of ions confirm that the state of an isolated ion significantly differs from the analogous state of the 'ionic' core of atoms of elements in their thermodynamically stable physical states.

Modern quantum-mechanical methods allow the electron energy in the individual shells to be determined more precisely than the Slater equation, nevertheless, the functional character of both remains the same.

5. Ionic radii

In materials science one generally deals with inorganic solids, with ionic or ionic -covalent bonds linking the components of their structures. The ionic radius is meaningless in quantum chemistry, nevertheless, it can be a useful working hypothesis to determine the space occupied by an ion in a crystal lattice. The division of the distance between ions depends on the applied method of calculation of ionic radii. The size of this space depends on temperature due to vibrations of ions. Hence, the real 'ionic radius' is smaller than the radius of the space in which the ion is situated. The difference can be estimated on the basis of thermal expansion coefficients or by using the so-called integral expansion [16]. Based on these data, one can estimate that the relative change in the radii of ions in the temperature range of 0–298 K is smaller than 1%, i.e., within the error limits of ionic radius estimation. As mentioned above, the ionic 'radius' is a characteristic value for a given ion and depends mainly on the 'radius' of the outermost shell. The size of this radius will also depend on interactions of ions (positive and negative) as well as on the repulsion of electronic shells. These effects will largely depend on the number of the nearest neighbours, the latter (coordination number) depending mainly on the relative sizes of the ions forming the crystal. Interactions between ions also result in their polarization, due to which the interaction energy increases and hence the ionic radii decrease. The problem of 'ionic radius' is thus very complex and its magnitude can vary depending on the type of the compound.

Despite the above reservations concerning the ionic radii, we decided in the present work to proceed with the analysis, assuming that the ionic radii given in reference books have been repeatedly discussed and can consequently be regarded as verified. For the analysis were used the so-called Pauling's [4, 7, 17] and Shannon's ionic radii [4, 7, 18, 19], at present regarded as being the most reliable. The dependences of the reciprocal radii of ions of coordination number $n = 6$ on the nuclear charge of ion is depicted in Fig. 4 for a number of electron configurations.

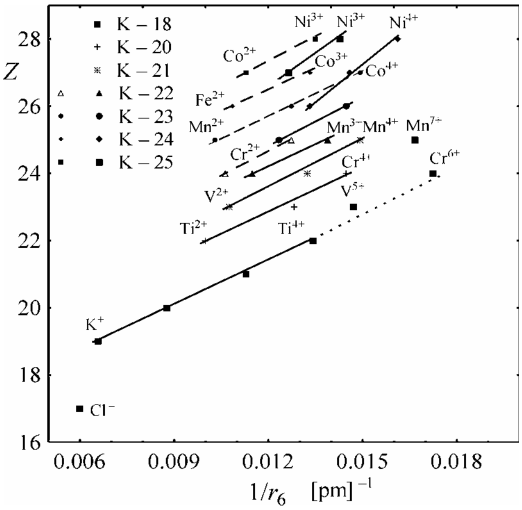

Fig. 4. Correlation between the nuclear charge of an ion and the reciprocal of radii of ions of coordination number $n = 6$, for 18-(K–18), 20–25-(K–20 to K–25)-electron configurations. Open points denote the $1/r$ values for high-spin ions

As can be noticed, the dependences of the reciprocal of the ionic radius on the nuclear charge of ion are linear and have similar slopes not only for ions of argon atom configuration (with a filled (sp) shell) but also for ions of other configurations (incompletely filled (d) subshells). Only two configurations K–24 (Fe^{2+}–Ni^{4+}) and K–25 (Co^{2+}–Ni^{3+}) for ions of low spin states deviate from the pattern, whereas the lines for these ions in high spin states are parallel to the other lines. It is worth noting that while in the case of V^{5+} and Cr^{6+} ions only a small deviation occurs from the line determined for other ions of K–18 configuration, the $1/r_6$ value for manganese Mn^{7+} ion shows a significant deviation from the determined line. Since the lines for electron configurations for ions containing more than 18 electrons are based on two or three values of ionic radii, considerable errors for the estimation of these parameters can be expected. Nonetheless, the slope, close to that of the line determined for cations of 18-electron configuration, justifies the correctness of the assumed relationships. Figure 5 presents the dependences of reciprocal ionic radii on the nuclear charge of ions for various coordination numbers. In Figure 5a, the above relationship is illustrated for configurations of the electron number $N_c = 2, 10, 12$; in Fig. 5b, for 18–25 electron configurations, and in Fig. 5c, for 28, 34 and 46-electron configurations. As can be seen in the figures, the points of the discussed relationship lie on straight lines for ions of respective coordination numbers, nonetheless, their slopes exhibit quite large differences. It is worth noting that the radius of C^{4+} carbon ion of coordination number $n = 4$ is bigger than the radius of B^{3+} ion and shows a considerable deviation from the line determined for ions of the tetrahedral configuration (Fig. 5a). Similarly, Al^{3+} ion has the same radius as the magnesium ion and also demonstrates a significant deviation from the line determined for ions of the tetrahedral configuration. Its radius is close to that of the ion of the octahedral configuration. This demonstrates that these ions have relatively larger radii than cations of the same configuration. It can be generally concluded that cations of the charge higher than four systematically exhibit a deviation from the line determined for cations of a small charge. This deviation from the linear relationship can therefore be related to an increasing contribution of the covalent bonding to the interactions between atoms.

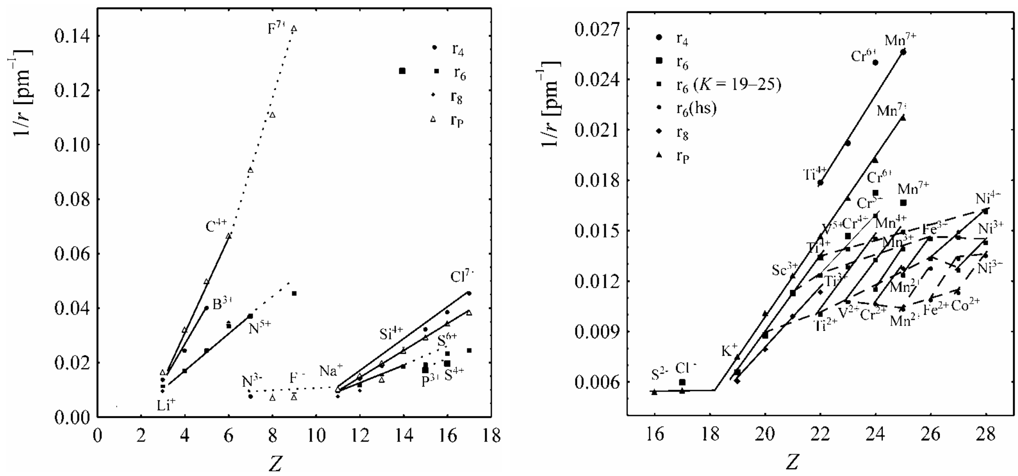

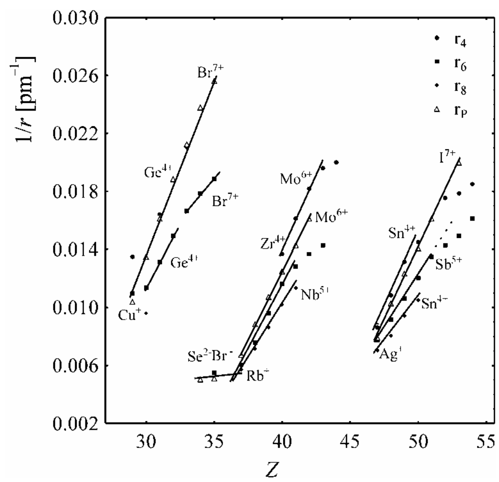

Fig. 5. Dependence of reciprocal radii of ions of coordination numbers $n = 4, 6, 8$ and Pauling's radii on the nuclear charge of ions. The subscript at the radius symbol r_n denotes the value of coordination number, r_P – Pauling's radius: a) for ions of He (K–2) and Ne (K–10) atom electron configuration (open points), the points (□) – for 12-electron configuration, b) for 18-electron (filled points) and 19–25-electron (□) configurations, (○) high spin state, c) for configurations of Ni-(K–28), Pd-(K–46) and Pt-(K–78) atoms

A substantial deviation of the $1/r_a$ value for anions from the line determined for cations of the same electron configuration (Fig. 5) is somewhat surprising. If the correlations were correct, the radii of anions should be considerably bigger than estimated. Smaller radii of anions can be due to a contribution of covalent interactions between cations and anions, as well as between anions. It should be noted that the radii of dinegative ions and even the radius of the trinegative nitrogen ion are not considerably smaller than the radii of mononegative ions. This feature indicates that the participation of covalent interaction in the bonding with these anions is even larger. The situation is thus opposite to the case of isolated anions of halogens, in which a decrease in the interaction energy of the last electron was observed, which is equivalent to an increase in the radius of the isolated ion. It can therefore be assumed that the anions in crystals behave as ions of a higher hypothetical nuclear charge, thus a higher atomic number should be assigned to them.

The linear character of the relationship between the reciprocal of ionic radii and the atomic number for a number of ions of a given configuration allows the parameters of the straight line to be determined according to the equation:

$$Z = \frac{a_r}{\frac{r}{a_0}} + S_r \tag{5}$$

The radii of ions are expressed in terms of atomic units of length after dividing them by the radius of the first hydrogen atom orbit ($a_0 = 5.29\times10^{-9}$ cm). The straight-line parameters were determined for the points randomly arranged alongside a straight line. The correlation coefficient for the obtained linear function was $R = 0.99975$.

Figure 6a presents the dependence of the parameter a_n on the number of electrons in the given electron configurations for ions of the coordination numbers $n = 4$ and 8, as well as for Pauling's ionic radii. They were also compared to the analogous parameters of the straight lines based on ionisation of the corresponding ions of the same configuration. The series of ions of the same electron configuration which were taken for computing the straight-line parameters are marked by the symbols of the elements next to the plotted points. As can be seen, the character of the relationship is similar to the analogous relationship based on ionisation enthalpies. A monotonous increase in the parameter a_n with the number of electrons in the configuration is observed and, for the respective coordination numbers, this relation can be described with two or three linear functions. Due to a relatively high number of ions of coordination number $n = 6$ and of various electron configurations, an analogous comparison of the dependence of parameters a_{IE} and a_6 on the number of electrons of the ion electron configuration is presented in Fig. 6b. As can be seen in the above figure, the values of the parameter a_n are arranged in a relatively narrow range for a majority of electron configurations, practically along the broken line. A certain deviation occurs for configurations with over 22 electrons, particularly for the 24- and 25-electron configurations mentioned previously, as well as for 38–42- and 68-, 70- and 72-electron configurations. The points entering the correlation were determined based on two or three values of ionic radii, hence the above deviations can hardly be ascribed to erro-

Table 2. Parameters a_n and S_n^* of Eq. (5) for ions of the same electronic configuration of N_c electrons

Configu-ration	N_c	Ions	a_4	S_4	Ions	a_6	S_6	Ions	a_8	S_8	Ions	a_P	S_P
1	2	3	4	5	6	7	8	9	10	11	12	13	14
$1s^2$	2	Li^+–B^{3+}	1.420	2.043	Li^+–N^{5+}	2.735	1.445				Li^+–C^{4+}	1.126	2.033
$1s^2$	2										N^{5+}–F^{7+}	0.716	3.646
2(sp)	10	Na^+–Cl^{7+}· $(Al^{3+})^{**}$	3.063	9.763	Na^+–Si^{4+}	5.734	8.436	Na^+–Mg^{2+}	8.860	7.448	Na^+–Cl^{7+}	4.024	8.748
2(sp)	10	O^{2-}–F^-	38.913	–8.602							O^{2-}–F^-	89.951	–26.000
$3s^2$	12				P^{3+}–S^{4+}	8.363	7.714						
3(sp)	18	Ti^{4+}–Mn^{7+}· (Cr^{6+})	5.609	16.941	K^+–Ti^{4+}	8.973	15.8	K^+–Ti^{4+}	10.533	15.586	K^+–Mn^{7+}	8.073	15.739
3(sp)	18										S^{2-}–Cl^-	209.784	–44.333
$3(sp)d^1$	19	Cr^{5+}–Mn^{6+}	4.022	19.611	Ti^{3+}–Cr^{5+}	10.659	15.083	V^{4+}–Cr^{5+}	7.692	18.267			
$3(sp)d^2$	20	Cr^{4+}–Mn^{5+}	6.106	18.125	Ti^{2+}–Cr^{4+}	8.233	17.581						
$3(sp)d^3$	21				V^{2+}–Mn^{4+}	8.945	17.859						
$3(sp)d^4$	22				Cr^{2+}–Mn^{3+}	7.891	19.2						
$3(sp)d^4$ (hs)	22				Cr^{2+}–Mn^{3+}	8.996	18.935						
$3(sp)d^5$	23				Mn^{2+}–Fe^{3+}	8.801	19.25						
$3(sp)d^5$ (hs)	23				Mn^{2+}–Co^{4+}	8.180	20.521						
$3(sp)d^6$	24				Fe^{2+}–Ni^{4+}	13.478	16.525						
$3(sp)d^6$ (hs)	24				Fe^{2+}–Co^{3+}	7.670	21.588						
$3(sp)d^7$	25				Co^{2+}–Ni^{3+}	11.611	19.222						
$3(sp)d^7$ (hs)	25				Co^{2+}–Ni^{3+}	8.535	21.897						
$3(sp)d^{10}$	28	Zn^{2+}–Ge^{4+}	7.045	24.939	Zn^{2+}–Ge^{4+}	10.611	23.615				Zn^{2+}–Br^{7+}	7.659	24.446
$3(sp)d^{10}$	28	As^{5+}–Br^{7+}	8.127	23.893	As^{5+}–Br^{7+}	14.280	20.594						
$4s^2$	30				Ge^{2+}–Se^{4+}	9.073	26.437						
4(sp)	36	Zr^{4+}–Mo^{6+}	8.410	33.878	Rb^+–Nb^{5+}	9.987	33.896	Rb^+–Nb^{5+}	13.134	33.016	Rb^+–Mo^{6+}	10.179	33.281

Table 2 cont.

1	2	3	4	5	6	7	8	9	10	11	12	13	14
4(sp)	36										Se^{2-}–Br^{-}	243.207	–31.000
$5s^2$	38				Nb^{3+}–Tc^{5+}	19.986	28.674						
$4(sp)d^3$	39				Mo^{3+}–Ru^{5+}	16.985	31.324						
$4(sp)d^4$	40				Ru^{4+}–Rh^{5+}	14.157	34.143						
$4(sp)d^5$	41				Ru^{3+}–Rh^{4+}	14.334	34.750						
$4(sp)d^6$	42				Ru^{3+}–Pd^{4+}	22.971	29.900						
$4(sp)d^{10}$	46	Ag^{+}–Sn^{4+}	9.608	42.489	Ag^{+}–Sb^{5+}	13.125	41.62	Ag^{+}–Sn^{4+}	15.938	41.106	Ag^{+}–I^{7+}	9.593	42.845
5(sp)	54				Cs^{+}–La^{3+}	12.565	51.402	Cs^{+}–Ce^{4+}	15.271	50.756	Cs^{+}–Ce^{4+}	14.239	50.487
5(sp)	54										Te^{2-}–I^{-}	180.341	8.800
$5s^2p^6$	68				Yb^{2+}–Ta^{5+}	13.036	64.051	Yb^{2+}–Ta^{5+}	15.701	63.516			
$5s^2p^7$	68	Hf^{4+}–Re^{7+}· (Ta^{5+})	10.370	64.342	Hf^{4+}–Re^{7+}	18.254	60.695						
$6s^2d^0$	70				Ta^{3+}–Os^{6+}	18.079	61.916						
$6s^2d^2$	72				Os^{4+}–Ir^{5+}	17.219	64.167						
$5(sp)d^{10}$	78	Hg^{2+}–Pb^{4+}	10.452	74.919	$Hg^{2+}Pb^{4+}$	13.164	74.243	Hg^{2+}–Tl^{3+}	17.124	72.941	Au^{+}–Bi^{5+}. (Hg^{2+})	12.219	74.260
$5(sp)d^{10}$	78				Bi^{5+}–At^{7+}	18.018	72.241						
$6s^2$	80				Tl^{+}–Po^{4+}	17.574	75.194	Tl^{+}–Bi^{3+}	19.766	74.885			
6(sp)	86				Fr^{+}–U^{6+}	14.273	83.045	Ra^{2+}–Pa^{5+}	16.922	82.473			
$7s^2$	88				Pa^{3+}–Pu^{6+}	16.066	83.747						

*Subscript *n* at constants denotes the values obtained by means of Pauling's radii (p) and Shannon's ionic radii for ions of coordination numbers *n* = 4, 6 and 8.

**( ) The ions, whose radii values have not been taken in calculation of the parameters of linear functions.

neous values of the ionic radii. The deviations can be related to ions of higher charge, mainly to 3d, 4d and 5d transition metal ions.

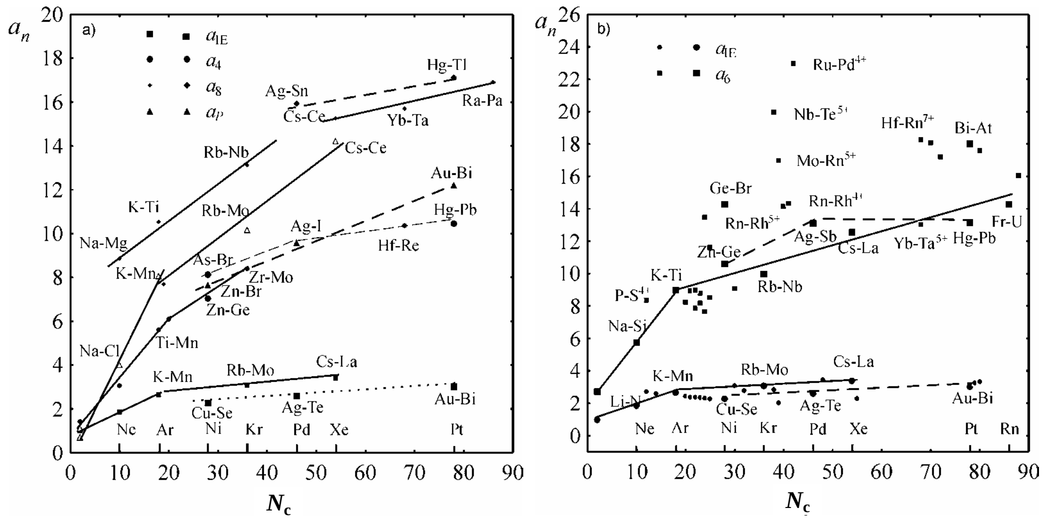

Fig. 6. Dependence of the parameter a_n in Eqs. (1) and (5) on the number of electrons in ions of respective configurations: a) for ions of coordination number $n = 4$, 8 and Pauling's radii; the electron configurations of Ni, Pd and Pt atoms are denoted with filled points, b) for ions of coordination number $n = 6$. The electron configurations of filled shell ions (sp) (rare gas atoms) and subshell (d) (Ni, Pd and Pt atoms) are denoted with filled points

As the ionisation energies and the ionic radii characterise similar ions, the parameters in Eqs. (1) and (5) should be functionally related. Determining the ionic radii, Pauling assumed that the atom radius depends on the most probable distance of the outer (valence) electrons from the nucleus and that it is inversely proportional to the effective nuclear charge. Slater [13–15] postulated an analogous relationship for calculating atomic shell radii, showing that the maximum of the radial function occurs at the distance r equal to:

$$r = \frac{\left(n^*\right)^2 a_0}{Z - S_S} \tag{6}$$

Rearranging Eq. (6), we obtain the equation:

$$Z = \frac{(n^*)^2}{\frac{r}{a_0}} + S_S \tag{7}$$

which is of an analogous type as the obtained experimental relationships (Eq. (5)). Thus, comparing the experimental relationships, (1) and (5), and the Slater equations, (4) and (7), we can see that if the ionisation enthalpy and ionic radii are expressed in atomic units, then the following relation should exist between the coefficients in the above equations:

$$n^{*} \cong a_{\mathrm{IE}} = \sqrt{a_r} \tag{8}$$

Dependence of a_{IE} and $\sqrt{a_r}$ on the number of electrons of respective electron configurations of ions is presented in Fig. 7. Taking into account the fact that Eqs. (4) and (7) are approximate, the agreement seems to be very good, both in the character of the equation and in the values of a_n themselves, in particular for ions of rare gas structure and ions of a small charge. As can be seen in Fig. 7, the dependence of $\sqrt{a_r}$ on the number of electrons in the configuration for given coordination numbers and a number of electron configurations of filled electron shells shows a much better linearity than that presented in Fig. 6. The remaining groups of ions, and in particular ions of a higher charge, deviate from the lines determined for the electron configurations mentioned above.

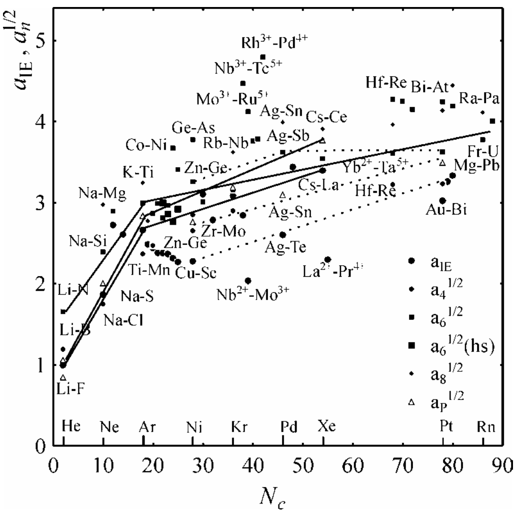

Fig. 7. Dependence of the parameters a_{IE} and $(a_n)^{1/2}$ in Eqs. (1) and (5) on the number of electrons in respective configurations. The points (■) denote the values of the parameter $a_6^{1/2}$ for ions of the coordination number $n = 6$ in their high spin states

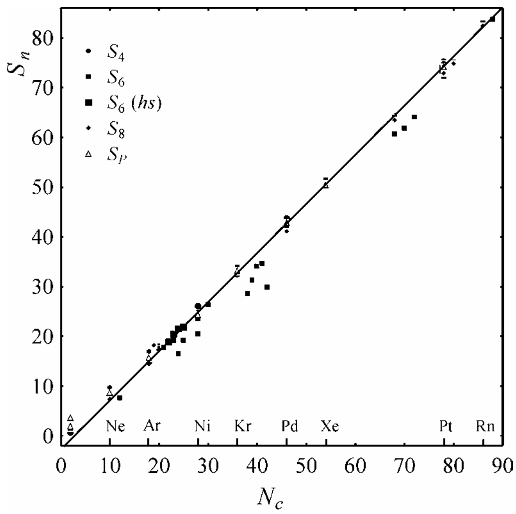

Fig. 8. Dependence of the S_n parameters on the number of electrons of respective configurations for ions of coordination numbers $n = 4$, 6, 8 and Pauling's radii (S_P). The points (■) denote the ions in their high spin states. The straight line was plotted on the basis of the ionisation enthalpies of ions of filled electronic shells (Eq. (2))

Figure 8 presents the dependence of the parameter S_n on the number of electrons for the discussed electron configurations. The solid line represents the relationship calculated for the points based on ion ionisation enthalpy (Eq. (2)); the points used in the calculations have not been shown for clarity. As can be seen, the values of the parameter S_n agree quite well with the values of the parameters based on ion ionisation enthalpy, in particular for filled shell ions. Quite significant deviations, for instance in the case of the parameter a_n, occur for ions of 3d and 4d metals of a higher charge and of previously discussed configurations. A relatively good agreement is also observed between the parameter S_n and the values of the screening constant calculated according to the Slater rules.

6. Conclusions

The following conclusions can be drawn from the above analysis of the ion ionisation enthalpy and their radii:

A number of cations of the same electron configuration and of the charge of 1–4 and beyond demonstrate a linear relationship between the reciprocal of the ion radius or the square root of their ionisation enthalpy and the nuclear charge of the ion (atomic number).

The agreement between the relations determined experimentally and the Slater equations describing the radius of an electronic shell and the electron energy in that shell demonstrates that the coefficients a_{IE} and $(a_n)^{1/2}$ as well as S_n in Eqs. (1) and (5) can be referred to as the 'experimental' effective principal quantum number and the 'experimental' screening constant, respectively, and the difference $(Z - S_n)$ can be called the 'experimental' effective nuclear charge of the ion. These values can be applied to characterise the ions.

As expected, it results from the analysis of the parameters of experimental equations of the type (1) and (5) that the states of isolated ions and ions in crystals described on the basis of ionisation energies, electron binding energies and ionic radii are different. In particular, significant differences occur in the case of ions having electrons in the (d) subshell. The state of the analogous 'ion' core in atoms of metals is also considerably different.

References

[1] SLATER J.C., *The Self-Consistent Field Method for Molecules and Solids*, McGraw-Hill, New York, 1974, Vol. 4.
[2] PEARSON R.G., *Chemical Hardness*, John Wiley, New York, 1997.
[3] LEVY M., PERDEW J.P., Phys. Rev. A, 32 (1985), 2010.
[4] HUHEEY J.E., KEITER E.A., KEITER R.L., *Inorganic Chemistry: Principles of Structure and Reactivity*, 4th Edition, Harper Collins, New York, 1993.
[5] *Handbook of Chemistry and Physics,* 79th Edition, D.R. Lide (Ed.), CRC Press, Boca Raton, Fl., USA, 1998.
[6] *Lange's Handbook of Chemistry*, 14th Edition, J.A. Dean (Ed.), McGraw-Hill, New York, 1992.
[7] WINTER M., WebElements: University of Sheffield, England (www.webelements.com).
[8] JAMES A.M., LORD M.P., *Macmillan's Chemical and Physical Data*, Macmillan, London, 1992.
[9] BEARDEN J.A., BARR A.F., *Rev. Mod. Phys.*, 39 (1967), 125.
[10] CARDONA M., LEY L. (Eds.), *Photoemission in Solids. I. General Principles*, Springer-Verlag, Berlin, 1978.

[11] FUGGLE J.C., MORTENSSON N., J. Electron Spectrosc. Relat. Phenom., 21 (1980), 275.
[12] WILLIAMS G. http:/pubweb.bnl.gor/people/gwyn/ebindene.html (www.webelements.com).
[13] SLATER J.C., Phys. Rev., 36 (1930), 57.
[14] SLATER J.C., *Quantum Theory of Atomic Structure*, McGraw-Hill, New York, 1960.
[15] MCWEENY R., *Coulson's Valence*, Oxford Univ. Press., Oxford, 1979.
[16] CHOJNACKI J., Bull. Acad. Polon. Sci., Ser. A 123 (1951), 321.
[17] PAULING L., J. Am. Chem. Soc., 49 (1927), 765.
[18] SHANNON R.D., Acta Cryst., A 32 (1976), 751.
[19] SHANNON R.D., PREWITT C.T., Acta Cryst., B 25 (1969), 925; B 26 (1970), 1046.

Received 13 June 2003
Revised 3 November 2003